Molecular Crystals and Liquid Crystals

ISSN: 1542-1406 (Print) 1563-5287 (Online) Journal homepage: http://www.tandfonline.com/loi/gmcl20

A new instrumentation for in situ characterization of the charge transport and crystallographic properties in co-evaporated organic thin film transistor

Takeshi Watanabe, Mamoru Kikuchi, Kousaku Nishida, Tomoyuki Koganezawa, Ichiro Hirosawa & Noriyuki Yoshimoto

To cite this article: Takeshi Watanabe, Mamoru Kikuchi, Kousaku Nishida, Tomoyuki Koganezawa, Ichiro Hirosawa & Noriyuki Yoshimoto (2016) A new instrumentation for in situ characterization of the charge transport and crystallographic properties in co-evaporated organic thin film transistor, Molecular Crystals and Liquid Crystals, 636:1, 168-175, DOI: 10.1080/15421406.2016.1201411

To link to this article: http://dx.doi.org/10.1080/15421406.2016.1201411

Published online: 01 Nov 2016.

Submit your article to this journal

Article views: 7

View related articles

View Crossmark data

Full Terms & Conditions of access and use can be found at
http://www.tandfonline.com/action/journalInformation?journalCode=gmcl20

Download by: [College of Business Education] **Date:** 24 December 2016, At: 01:18

MOLECULAR CRYSTALS AND LIQUID CRYSTALS
2016, VOL. 636, 168–175
http://dx.doi.org/10.1080/15421406.2016.1201411

Taylor & Francis
Taylor & Francis Group

A new instrumentation for *in situ* characterization of the charge transport and crystallographic properties in co-evaporated organic thin film transistor

Takeshi Watanabe[a], Mamoru Kikuchi[b], Kousaku Nishida[b], Tomoyuki Koganezawa[a], Ichiro Hirosawa[a], and Noriyuki Yoshimoto[b]

[a]Japan Synchrotron Radiation Research Institute, Sayo, Japan; [b]Graduate School of Engineering, Iwate University, Morioka, Japan

ABSTRACT

A new instrumentation was developed to study the *in situ* electrical and crystallographic properties of organic thin film transistor during vacuum deposition. We characterized pentacene (PEN) and perfluoro-pentacene (PFP) co-deposited organic thin film transistor with various mixing ratio using this equipment. Lattice parameters and crystal orientations of PEN and PFP alloyed phases (named σ-phase and λ-phase) were determined using an *in situ* two-dimensional grazing incidence X-ray diffraction (2D-GIXD) measurement. The observed 2D-GIXD patterns clarified that the σ-phase is in triclinic unit cell with the following lattice parameters: $a =$ 0.67 nm, $b = 0.75$ nm, $c = 1.58$ nm, $\alpha = 95.7°$ $\beta = 94.2°$ and $\gamma = 84.0°$. The c plane of σ-phase crystal is parallel to the substrate surface. The λ-phase is also in triclinic with the following lattice parameters: $a = 0.66$ nm, $b =$ 0.69 nm, $c = 1.56$ nm, $\alpha = 109.5°$ $\beta = 113.0°$ and $\gamma = 81.5°$. The a plane of λ-phase crystal was parallel to the substrate surface. It was also found the best symmetric hole and electron mobility ($\mu_h = 5.5 \times 10^{-4}$ $cm^2V^{-1}s^{-1}$ and $\mu_e = 5.1 \times 10^{-4}$ $cm^2V^{-1}s^{-1}$) were obtained at PEN: PFP = 1:1.

KEYWORDS

A vacuum deposition system for in situ X-ray diffraction and electrical measurements; Organic thin film transistors; Pentacene; Perfluoro-pentacene

Introduction

Crystallographic characterization of organic thin film such as grain size, crystal polymorphs, and crystal orientation is necessary for improving the performance of organic thin film transistors (OTFTs). The crystallographic characterization of OTFTs has been carried out in air generally. Recently, Mannebach *et al.* investigated not only the crystal orientation and polymorphs but also transport property within the channel region of OTFTs in air [1]. However, the organic semiconductor material is susceptible to the oxidative degradation by exposed to light and air [2–4]. Therefore, *in situ* electrical and crystallographic studies without the air exposure and wetting are necessary.

Co-deposited thin films have attracted attention because of their application for organic device including organic solar cells and organic ambipolar transistors [5–7]. It was reported that PEN and PFP co-deposited thin film works as an ambipolar OTFT [7]. Salzmann *et al.* and Hinderhofer *et al.* also proposed that it forms two types of alloyed phases named

CONTACT Takeshi Watanabe t5511001@spring8.or.jp Japan Synchrotron Radiation Research Institute, Sayo, Japan.
Color versions of one or more of the figures in the article can be found online at www.tandfonline.com/gmcl.
© 2016 Taylor & Francis Group, LLC

"σ-phase" and "λ-phase" [8, 9]. However, their crystal structures, even their lattice parameters, are unclear.

In this work, we developed a new instrumentation which enables to investigate the charge transport and crystallographic properties of organic semiconductor without air exposure. We also characterized co-deposited PEN and PFP OTFTs.

Instrumentation and experimental

(1) Instrumentations

In situ electrical and crystallographic characteristics of OTFT were conducted using home-made portable deposition chamber schematically shown in Figure 1. The chamber can be mounted to multi-axes diffractometer with low loads because it has lightweight (<15 kg) and compact size (160 mm × 160 mm × 400 mm). Two beryllium windows for X-ray transmission and three electric current feedthroughs were attached to the sample stage. The chamber is equipped with deposition cells, beryllium windows and sample stage for *in situ* X-ray diffraction. Small size of Kundsen cells (K-cells: ϕ12 mm ×31 mm) were installed. The co-deposition is performed by remote controlling two K-cells, two quartz crystal microbalances and three shutters.

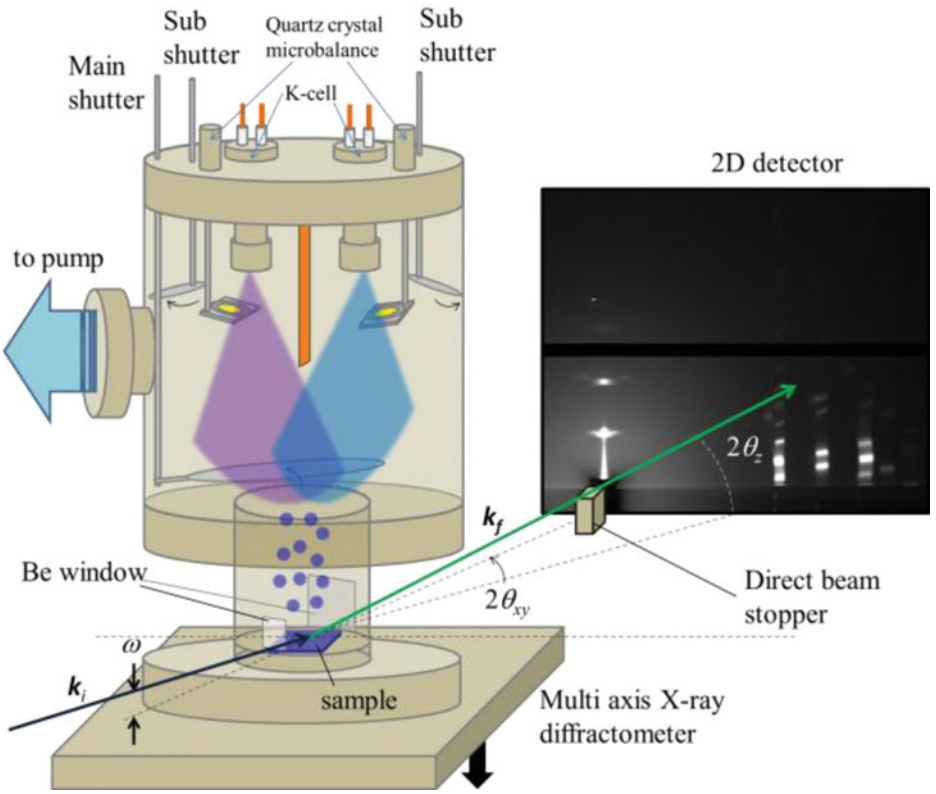

Figure 1. Schematic geometry of vacuum deposition chamber for *in situ* 2D-GIXD measurement.

(2) Experimental conditions

In situ two-dimensional grazing incidence X-ray diffraction (2D-GIXD) measurements were performed at BL19B2 beamline in SPring-8 using a multi-axes diffractometer and large area detector (PILATUS 300K) combined with a home-made portable deposition chamber [10–12]. PEN (Sigma Aldrich, triple-sublimed grade 99.995% purity) and PFP (Kanto Denka Kogyo Co., 99% purity) was vacuum co-deposited onto silicon wafer coated with native silicon oxide (SiO_2). The deposition rate was 0.005 nm/s and the film thickness was 0∼30 nm. The substrate temperature and mixing ratio of PEN and PFP were 25°C and 1:0 (pristine PEN), 0:1 (pristine PFP), 1:1, 2:1 (PEN rich), and 1:2 (PFP rich). The mixing ratio was controlled by quartz crystal microbalance. The base pressure was 2.0×10^{-4} Pa. X-ray energy for this experiment is 12.40 keV. The highly brilliant and collimated synchrotron X-ray was irradiated on the substrate surface with a grazing angle of $\omega = 0.12°$. Integration time for photon counting on the x-ray detector was 30 s for each image, and the total number of the acquired images was 200 frames for each measurement. The distance between the sample and the detector was calibrated to be 174 mm with polycrystalline LaB_6. The unit-cell parameter was calculated via a procedure described elsewhere [13].

Highly p-doped silicon wafer (gate electrodes) covered with thermal silicon dioxide (300 nm insulator) was used as a substrate. Thickness of organic semiconductor layer was 30 nm. The Au source and drain electrodes (channel length $L = 40$ μm, channel width $W = 5$ mm) were evaporated through a shadow mask. Current–voltage characteristics were obtained 25°C in vacuum.

Result and discussion

A. PEN:PFP = 1:1

Figure 2 shows the *in situ* 2D-GIXD patterns of co-deposited thin film. The take-off and horizontal components of scattering angle are denoted as $2\theta_z$ and $2\theta_{xy}$ respectively. At the beginning of the deposition (Figure 2(a)), a fainted diffraction spot appeared at $2\theta_{xy} = 15.7°$ and 17.7°. These patterns are not attributed to pristine PEN and PFP. With increasing thickness to 15 nm (Figure 2 (b)), this diffraction became more intense and other diffraction spots appeared at $2\theta_{xy} = 7.8°$, 8.7° and 12.1°. All observed diffraction spots could be explained as alloyed σ-phase reported in previous studies [8, 9, 14]. The spot patterns also indicate that this co-deposited thin film is highly oriented along surface normal. In the film of 15 nm in thick, diffraction spots come from λ-phase newly appeared (marked by grey arrows in Figure 2 (c)). This result suggested that PEN and PFP alloyed σ-phase is occurs in early stage of co-deposition, and then λ-phase appeared over 30 nm. The pristine PEN film is well known that the metastable "thin film phase" preferentially forms in early stage of deposition and then the stable "bulk phase" occurs with increasing film thickness [10, 15–19]. The observed polymorphic behavior of co-evaporated thin film is similar to that of the pristine PEN.

The unit cell parameters and crystal orientation were determined from observed diffraction patterns. Figure 3 shows the comparison of experimental and calculated (marked by open circles) 2D-GIXD patterns. The calculated $2\theta_{xy}$ and $2\theta_z$ based on lattice parameters listed in Table 1 matched well to observed ones, as shown in Table 2. It can be concluded that σ-phase is in triclinic unit cell with the following lattice parameters: $a = 0.67$ nm, $b = 0.75$ nm, $c = 1.58$ nm, $\alpha = 95.7°$ $\beta = 94.2°$ and $\gamma = 84.0°$. The c plane of σ-phase crystal is parallel to the substrate surface. As for λ-phase, it has also a triclinic unit cell with the following lattice parameters: $a = 0.66$ nm, $b = 0.69$ nm, $c = 1.56$ nm, $\alpha = 109.5°$ $\beta = 113.0°$ and $\gamma = 81.5°$. It is found that a plane of λ-phase crystal is parallel to the substrate surface. The unit cells of

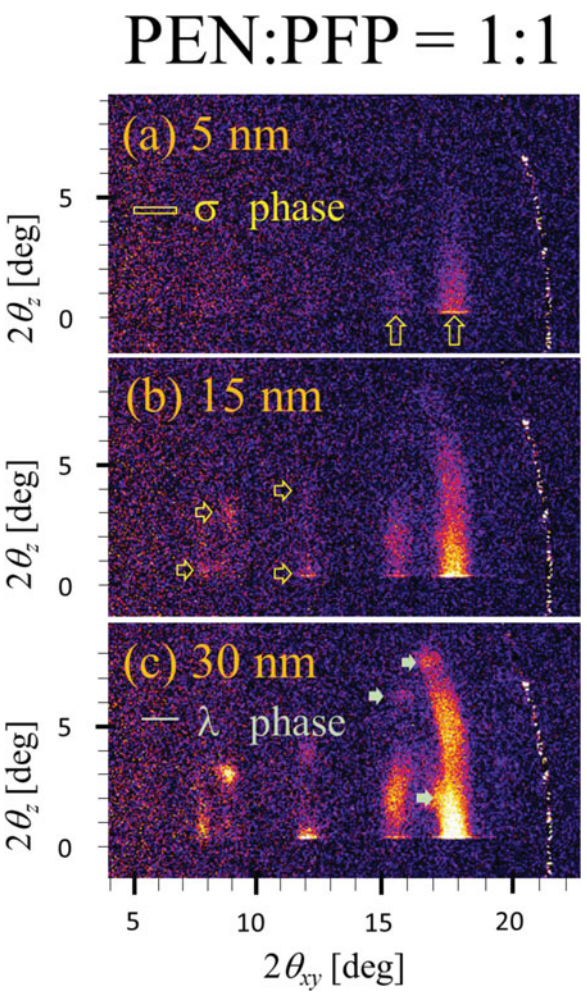

Figure 2. *In situ* 2D-GIXD patterns of co-evaporated PEN: PFP = 1:1. The images are shown for film thickness of (a) 5 nm, (b) 15 nm and (c) 30 nm. Labeling: yellow allows: alloyed σ-phase and grey allows: alloyed λ-phase.

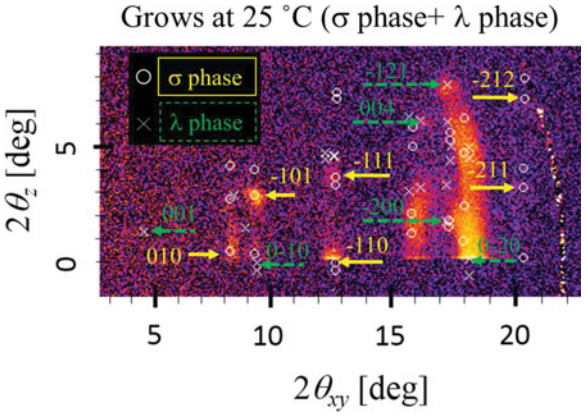

Figure 3. Comparison of the experimental and the calculated 2D-GIXD patterns of co-deposited PEN: PFP = 1:1. The white circles and crosses show the result of calculations. Some of the intense diffractions are indexed and labeled on the figure.

Table 1. Lattice parameter of alloyed crystals, pristine PEN and PFP crystals. The unit cell parameters of pristine PEN and pure PFP were referred in Refs 17, 18, 20 and 21.

	a (nm)	*b* (nm)	*c* (nm)	α (deg)	β (deg)	γ (deg)
Alloyed (σ-phase)	0.67	0.75	1.58	95.7	94.2	84
Alloyed (λ-phase)	0.66	0.69	1.56	109.5	113.0	81.5
PEN (Thin film)	0.59	0.76	1.57	98.6	93.3	89.8
PEN (Bulk)	0.61	0.79	1.58	112.7	101.3	85.7
PFP (Thin film)	1.14	0.45	3.10	90	91.6	90
PFP(Bulk)	1.15	0.45	1.55	90	91.6	90

Table 2. The comparison of experimental and calculated $2\theta_{xy}$ and $2\theta_{z}$. The experimental $2\theta_{z}$ of 1–10 (σ-phase), 0–10 (λ-phase) and 0–20 (λ-phase) marked by "$*$" are expressed to be 0.26° corresponding to the Yoneda peaks of their crystal truncation rods.

	hkl	$2\theta_{xy\_cal}$ (deg)	$2\theta_{z\_cal}$ (deg)	$2\theta_{xy\_exp}$ (deg)	$2\theta_{z\_exp}$ (deg)
σ-phase	010	7.8	0.6	7.7 ± 0.2	0.7 ± 0.4
	−101	8.7	2.9	8.8 ± 0.2	3.0 ± 0.2
	−110	12.1	0.03	12.0 ± 0.2	0.26*
	−111	12.1	3.7	12.0 ± 0.2	3.6 ± 0.5
	−211	19.9	3.1	19.7 ± 0.5	3.0 ± 0.2
	−212	19.8	6.8	19.5 ± 0.2	6.8 ± 0.3
λ-phase	001	3.9	1.4	3.9 ± 0.2	1.6 ± 0.2
	0–10	8.8	0.1	9.0 ± 0.2	0.26*
	004	15.7	6.0	15.8 ± 0.3	6.1 ± 0.2
	0–21	16.7	1.8	16.5 ± 0.6	1.9 ± 0.4
	0–20	17.6	0.2	17.7 ± 0.3	0.26*
	12–1	16.8	7.5	16.8 ± 0.5	7.6 ± 0.3

these alloyed phases and the pristine PEN and PFP are shown in Figure 4. The results show that the lattice parameters and preferred orientation of the σ-phase and the thin film phase of PEN resemble each other.

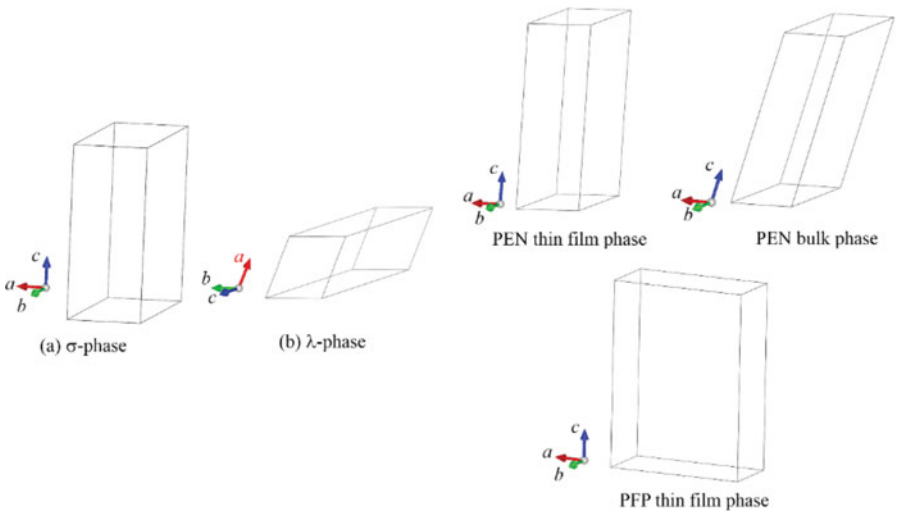

Figure 4. The schematically unit cell of (a) pristine PEN, (b) PFP, the alloyed (c) σ-phase and (d) λ-phase. The *c* face of the alloyed σ-phase, PEN thin film phase, bulk phase and PFP thin film phase are parallel to the substrate surface. The *a* face of the λ-phase is also parallel to the substrate surface.

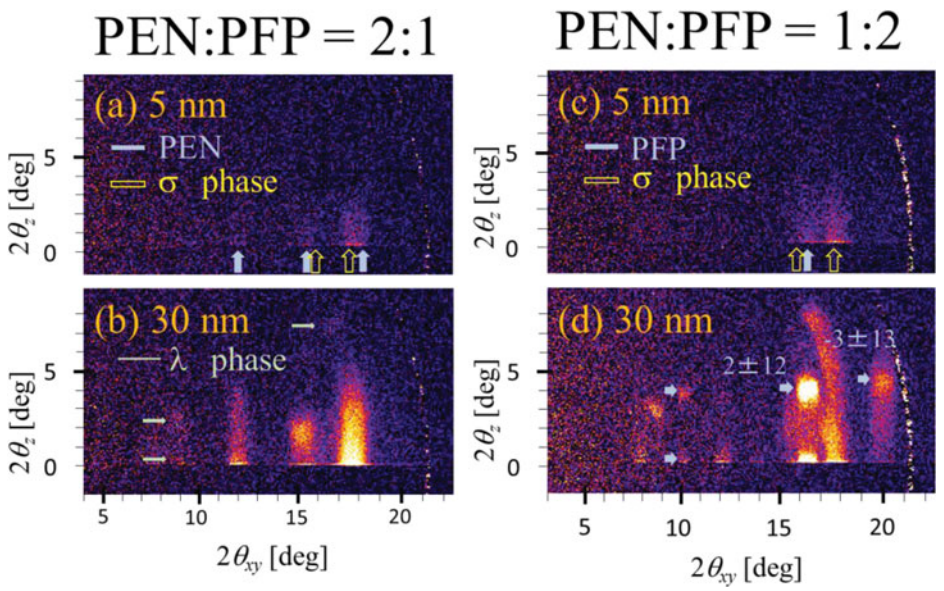

Figure 5. *In situ* 2D-GIXD patterns of co-evaporated PEN: PFP = 2:1 (left) and 1:2 (right). The images are shown for film thickness of (a) 5 nm, (b) 30 nm. Labeling: yellow allows: alloyed σ-phase, grey allows: alloyed λ-phase and blue allows: pristine PEN or PFP thin film phase.

Table 3. Hole and electron mobilities of co-deposited films with various mixing ratio.

PEN:PFP	1:0	2:1	1:1	1:2	0:1
$\mu_{p,max}$($cm^2V^{-1}s^{-1}$)	5.8×10^{-2}	1.4×10^{-5}	5.5×10^{-4}	5.7×10^{-6}	
$\mu_{n,max}$($cm^2V^{-1}s^{-1}$)		3.5×10^{-8}	5.1×10^{-4}	9.0×10^{-6}	1.9×10^{-3}

B. PEN:PFP = 2:1 and 1:2

Figure 5(a) and (b) show *in situ* 2D-GIXD patterns of PEN rich co-deposited thin film. The 2D-GIXD pattern with a film thickness of 5 nm (Figure 5 (a)) shows some diffraction explained to the σ-phase. A diffraction of PEN thin film phase appeared simultaneously at $2\theta_{xy} = 12.2^{\circ}$ with increasing thickness. It indicates that the PEN rich film was formed with alloyed and pristine PEN crystal phases. These intensities increased and some new diffractions coming from λ-phase were observed in 30 nm (Figure 5 (b)). It is worth noting that the PEN bulk phase does not appear over 30 nm in co-deposited film. In the case of PFP rich film, the alloyed and pristine PFP phase appeared and polymorphs of alloyed crystal transform from σ-phase to λ-phase (Figure 5 (c) and (d)). A schematic composition phase diagram of PEN and PFP co-deposited thin film was summarized shown in Figure 6 (a) and (b).

C. Ambipolar OTFTs characteristics

Figure 7 shows a transfer (left) and output (right) characteristics of PEN: PFP = 1:1 OTFTs. The device worked as an ambipolar transistor. The field effect mobility was extracted from $I_{ds} = \mu_h$ (or μ_e) $(WC_{OX}/2L)$ $(V_g - V_{th})^2$, where I_{ds} and C_{OX} are the drain-source current and the gate insulator capacitance, respectively. extracted from $I_{ds} = \mu_h$ $(WC_{OX}/2L)$ $(V_g - V_{th})^2$, where I_{ds} and C_{OX} are the drain-source current and the gate insulator capacitance, respectively. All the hole and electron mobility of different mix ratio OTFTs are listed in Table 3. The best

symmetric hole and electron mobility ($\mu_h = 5.5 \times 10^{-4}$ $cm^2V^{-1}s^{-1}$ and $\mu_e = 5.1 \times 10^{-4}$ $cm^2V^{-1}s^{-1}$) were obtained at PEN: PFP = 1:1. It is worth noting that the hole mobility of PEN: PFP = 2:1 and the electron mobility of 1:2 were much lower than 1:1 respectively. These results suggest heterogeneity in the co-deposited films coexisting of alloyed σ-phase and pristine PEN or PFP thin film phase may be origin of much lower transports by increasing carrier scattering.

Conclusion

We demonstrated a new instrumentation to investigate the crystal structural properties and charge transport of organic semiconductor during a vacuum co-deposition. The unit cell parameters of two alloyed phases (σ-phase and λ-phase) were proposed from *in situ* 2D-GIXD experiment. Both σ-phase and λ-phase were indexed by triclinic unit cell. The

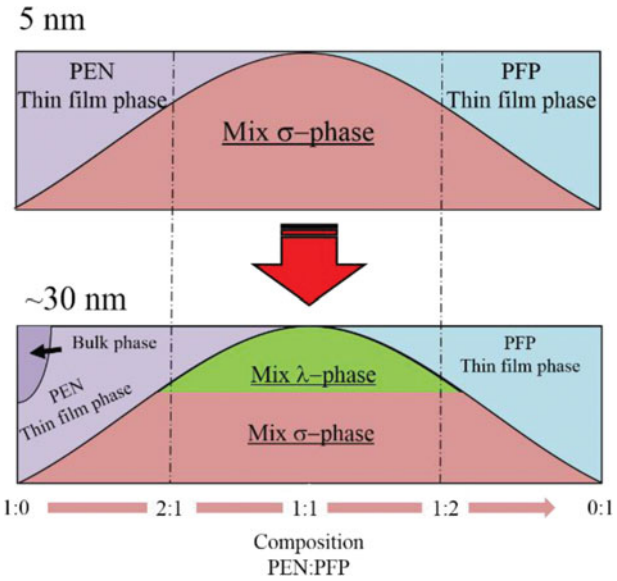

Figure 6. A schematic composition phase diagram of co-deposited thin film at 25°C. The film thickness are (a) 5 nm and (b) ~30 nm.

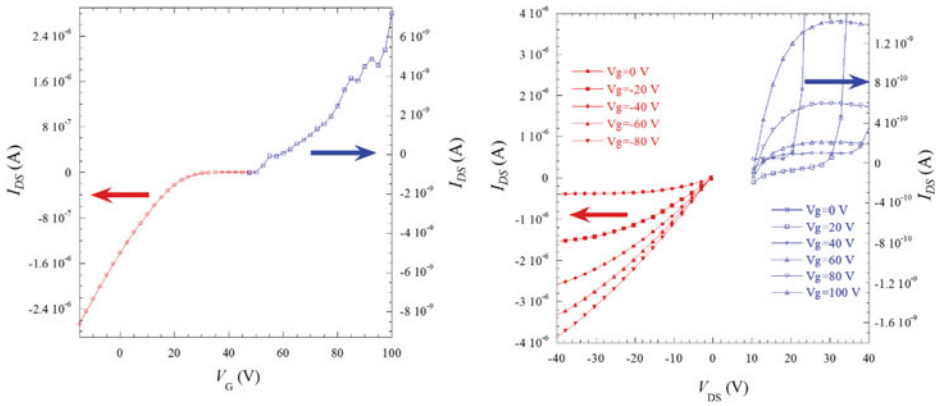

Figure 7. Electrical transfer (left) and output (right) characteristics of co-deposited PEN: PFP = 1:1 OTFTs.

σ-phase is oriented vertically to the substrate surface and the λ-phase was oriented parallel to the substrate surface. It found that the hole and electron transport occurs at the first few monolayer of alloyed σ-phase. The best symmetric hole and electron mobility were obtained at PEN: PFP = 1:1. This instrumentation is really effective to characterize the charge transport and crystal structural properties with minimizing the effect of the air.

Acknowledgments

The synchrotron radiation experiments were performed at BL19B2 in SPring-8 with the approval of Japan Synchrotron Radiation Research Institute (JASRI) (Proposal Nos. 2013A0036, and 2013B0036)

References

[1] Mannebach, E. M., Spalenka, J. W., Johnson, P. S., Cai, Z., Himpsel, F. J., & Evans, P. G. (2013). *Adv. Funct. Mater.*, *23*, 554.
[2] Vollmer, A., Weiss, H., Rentenberger, S., Salzmann, I., Rabe, J. P., & Koch, N. (2006). *Surface Science*, *600*, 4004.
[3] Lu, X., Minari, T., Kumatani, A., Liu, C., & Tsukagoshi, K. (2011). *Appl. Phys. Lett.*, *98*, 243301.
[4] Yang, H., Yang, L., Ling, M., Lastella, S., Gandhi, D. D., Ramanath, G., Bao, Z., & Ryu, C. Y. (2008). *J. Phys. Chem. C*, *112*, 16161.
[5] Hiramoto, M., Fujiwara, H., & Yokoyama, M. (1991). *Appl. Phys. Lett.*, *58*, 1062.
[6] Rost, C., Karg, S., Riess, W., Loi, M. A., Murgia, M., & Muccini, M. (2004). *Appl. Phys. Lett.*, *85*, 1613.
[7] Inoue, Y., Sakamoto, Y., Suzuki, T., Kobayashi, M., Gao, Y., & Tokito, S. (2005). *Jpn. J. Appl. Phys.*, *44*, 3663.
[8] Salzmann, I., Duhm, S., Heimel, G., Rabe, J. P., Koch, N., Oehzelt, M., Sakamoto, Y., & Suzuki, T. (2008). *Langmuir*, *24*, 7294.
[9] Hinderhofer, A., Frank, C., Hosokai, T., Resta, A., Gerlach, A., & Schreiber, F. (2011). *J. Chem. Phys.*, *134*, 104702.
[10] Watanabe, T., Hosokai, T., Koganezawa, T., & Yoshimoto, N. (2012). *Mol. Cryst. Liq. Cryst.*, *566*, 18.
[11] Hosokai, T., Watanabe, T., Koganezawa, T., Ackermann, J., Brisset, H., Videlot-Ackermann, C., & Yoshimoto, N. (2012). *MRS Proc.*, *1402*, 265.
[12] Toyokawa, H., Suzuki, M., Brönnimann, C., Eikenberry, E. F., Henrich, B., Hülsen, G., & Kraft, P. (2007). *AIP Conf. Proc.*, *879*, 1141.
[13] Watanabe, T., Koganezawa, T., Kikuchi, M., Ackermann, C. V., Ackermann, J., Brisset, H., Hirosawa, I., & Yoshimoto, N. (2013). *Jpn. J. Appl. Phys.*, *53*, 01AD01.
[14] Breuser, T., & Witte, G. (2013). *J. Chem. Phys.*, *138*, 114901.
[15] Schiefer, S., Huth, M., Dobrinevski, A., & Nickel, B. (2007). *J. Am. Chem. Soc.*, *129*, 10316.
[16] Kakudate, T., Saito, Y., & Yoshimoto, N. (2007). *Appl. Phys. Lett.*, *90*, 081903.
[17] Yoshida, H., & Sato, N. (2006). *Appl. Phys. Lett.*, *89*, 101919.
[18] Yoshida, H., Inaba, K., & Sato, N. (2007). *Appl. Phys. Lett.*, *90*, 181930.
[19] Kowarik, S., Gerlach, A., Hinderhofer, A., Milita, S., Borgatti, F., Zontone, F., Suzuki, T., Biscarini, F., & Schreiber, F. (2008). *Phys. Stat. Sol. (RRL)*, *2*, 120.
[20] Frank, C., Novác, J., Gerlach, A., Ligorio, G., Broch, K., Hinderhofer, A., Aufderheide, A., Banerjee, R., Nervo, R., & Schreiber, F. (2013). *J. Appl. Phys.*, *114*, 043515.
[21] Sakamoto, Y., Suzuki, T., Kobayashi, M., Gao, Y., Fukai, Y., Inoue, Y., Sato, F., & Tokito, S. (2004). *J. Am. Chem. Soc.*, *126*, 8138.